Journal of Zhejiang University SCIENCE B
ISSN 1673-1581 (Print); ISSN 1862-1783 (Online)
www.zju.edu.cn/jzus; www.springerlink.com
E-mail: jzus@zju.edu.cn

Influence of ginsenoside Rg1, a panaxatriol saponin from Panax notoginseng, on renal fibrosis in rats with unilateral ureteral obstruction*

Xi-sheng XIE[§1], Man YANG[1], Heng-cuang LIU[§2], Chuan ZUO[1], Zi LI[1], Yao DENG[1], Jun-ming FAN[†‡1,3]

([1]*Department of Nephrology, West China Hospital, Sichuan University, Chengdu 610041, China*)

([2]*Department of Medical Technology, West China School of Public Health, Sichuan University, Chengdu 610041, China*)

([3]*State Key Laboratory of Biotherapy of Human Diseases, West China Hospital, Sichuan University, Chengdu 610041, China*)

[†]E-mail: junmingfan2007@yahoo.com.cn

Received Jan. 20, 2008; revision accepted Apr. 26, 2008

Abstract: Total saponins of Panax notoginseng (PNS) have been shown to ameliorate renal interstitial fibrosis. Ginsenoside Rg1, a panaxatriol saponin, is one of the major active molecules from PNS. The present study was undertaken to investigate the effect of ginsenoside Rg1 on renal fibrosis in rats with unilateral ureteral obstruction (UUO). The rats were randomly divided into 3 groups: sham-operation (n=15), UUO (n=15) and UUO with ginsenoside Rg1 treatment (n=15, 50 mg per kg body weight, intraperitoneally (i.p.) injected). The rats were sacrificed on Days 7 and 14 after the surgery. Histological examination demonstrated that ginsenoside Rg1 significantly inhibited interstitial fibrosis including tubular injury as well as collagen deposition. α-smooth muscle actin (α-SMA) and E-cadherin are two markers of tubular epithelial-myofibroblast transition (TEMT). Interestingly, ginsenoside Rg1 notably decreased α-SMA expression and simultaneously enhanced E-cadherin expression. The messenger RNA (mRNA) of transforming growth factor-β1 (TGF-β1), a key mediator to regulate TEMT, in the obstructed kidney increased dramatically, but was found to decrease significantly after administration of ginsenoside Rg1. Further study showed that ginsenoside Rg1 considerably decreased the levels of both active TGF-β1 and phosphorylated Smad2 (pSmad2). Moreover, ginsenoside Rg1 substantially suppressed the expression of thrombospondin-1 (TSP-1), a cytokine which can promote the transcription of TGF-β1 mRNA and the activation of latent TGF-β1. These results suggest that ginsenoside Rg1 inhibits renal interstitial fibrosis in rats with UUO. The mechanism might be partly related to the blocking of TEMT via suppressing the expression of TSP-1.

Key words: Ginsenoside Rg1, Renal fibrosis, Tubular epithelial-myofibroblast transition (TEMT), Thrombospondin-1 (TSP-1), Transforming growth factor-β1 (TGF-β1)

doi:10.1631/jzus.B0820024 **Document code:** A **CLC number:** R692.6

INTRODUCTION

Renal interstitial fibrosis is the final common pathway of a wide variety of chronic kidney diseases (Liu, 2006). It is characterized by the accumulation of extracellular matrix (ECM) components including collagens I, III, and IV, proteoglycans and fibronectin. As far as the origin of matrix-producing cells in the kidney is concerned, several possibilities exist, including activation of resident interstitial fibroblasts, migrating haematopoietic or mesenchymal stem cells from the bone marrow, periadventitial cells, and tubular epithelial-myofibroblast transition (TEMT) (Strutz and Müller, 2006). Studies with genetic models have unambiguously illustrated that TEMT is emerging as a major pathway leading to generation of the matrix-producing cells in progressive renal fibrosis (Liu, 2004). We have reported that transforming growth factor-β1 (TGF-β1) is a key mediator to regulate TEMT (Fan *et al*., 1999). TGF-β1 and its downstream signaling molecule Smad2/3 activation play an important role in the

‡ Corresponding author
§ The two authors contributed equally to this work
* Project (No. 30170437) supported by the National Natural Science Foundation of China

progression of renal fibrosis (Wang *et al*., 2005). It is demonstrated that TGF-β1 is usually secreted as a latent procytokine complex that has to be activated before it can bind to its receptors. Thrombospondin-1 (TSP-1), a homeotrimeric multifunctional glycoprotein, has been identified as a major activator of TGF-β1 in experimental renal disease models and it is expressed in a number of kidney cell types, particularly in areas of tubulointerstitial injury (Yevdokimova *et al*., 2001; Hugo, 2003; Naito *et al*., 2004; Daniel *et al*., 2004). Specific strategies against TSP-1, such as anti-TSP-1 antisense oligonucleotides, markedly inhibited the activation of TGF-β1 and improved interstitial fibrosis (Daniel *et al*., 2003). These documents suggest that TSP-1-blocking therapies may contribute to renal interstitial fibrosis.

Panax notoginseng Buck F. H. Chen (Araliaceae) is one of the most widely used traditional Chinese herbal medicines for the treatment of coronary heart disease, cardiac angina, apoplexy, and atherosclerosis in clinics (Ng, 2006). Pharmacological studies showed that total saponins of Panax notoginseng (PNS) are the active components of this drug (Li *et al*., 2006). We have reported that PNS can block TEMT and inhibit the secretion of ECM, consequently ameliorating the fibrotic process of renal interstitium (Su *et al*., 2005; Wang *et al*., 2004). However, PNS is a compound of several saponins, and it remains unclear which components are the most effective saponins against renal fibrosis. Ginsenoside Rg1, a panaxatriol saponin, is one of the major active molecules from PNS. Distribution studies showed that, after oral or intravenous administration of PNS, ginsenoside Rg1 has a high concentration in kidney (Li *et al*., 2006). Besides, it is reported that, in a rat model with infarcted myocardium, ginsenoside Rg1 significantly attenuated the development of myocardial fibrosis (Wei *et al*., 2007). In a rat model with liver cirrhosis, by decreasing the expression of tumor necrosis factor-α and reducing the secretion of phospholipase A2, ginsenoside Rg1 could also improve hepatic fibrosis (Wu *et al*., 2003). The anti-fibrosis role of ginsenoside Rg1 in renal tubulointerstitial fibrosis remains to be clarified yet.

In the present study, we used the rat with unilateral ureteral obstruction (UUO), a model of renal fibrosis, to investigate the effects of ginsenoside Rg1 on renal impairment and the mechanisms involved.

MATERIALS AND METHODS

Animals

The studies were performed on male Sprague-Dawley (SD) rats (180~200 g) purchased from Laboratory Animal Center of Sichuan University (Chengdu, China). All rats in the study were used strictly in accordance with the National Institutes of Health Guide for the Care and Use of Laboratory Animals.

Experimental design

UUO was performed using an established procedure (Morrissey and Klahr, 1998; Guo *et al*., 2001). In brief, under intraperitoneal pentobarbital anesthesia, the left kidney and ureter were exposed via a flank incision. Then the left ureter was ligated with 4-0 silk at two points and cut between the ligatures in order to prevent retrograde urinary tract infection. Finally, the wound was closed in layers. Sham animals underwent identical surgical procedures, but the left ureter was simply manipulated.

Ginsenoside Rg1, whose chemical structure is shown in Fig.1 (Chan *et al*., 2002), was purchased from the Chinese National Institute for the Control of Pharmaceutical and Biological Products (Beijing, China). The animals that underwent surgery were randomly divided into three groups (n=15 per group): UUO group (UUO), sham-operation group (SOR) and ginsenoside Rg1 group (Rg1). Treatment started within 1 h after the surgical procedure. Rats in Rg1 group were injected intraperitoneally once daily with ginsenoside Rg1 50 mg per kg body weight (This dose had been shown to be potent in decreasing matrix accumulation in UUO model in the pilot study

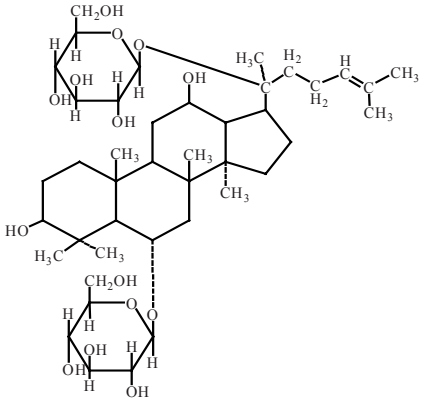

Fig.1 Chemical structure of ginsenoside Rg1

from our laboratory. In addition, no adverse effect was observed at this dose). UUO and SOR groups were injected intraperitoneally once daily with normal saline of the same volume. Six rats selected randomly from each group were sacrificed on Days 7 and 14 post-surgery, and the left kidneys were removed. The kidneys were sagittally sliced, snap frozen in liquid nitrogen and kept at −80 °C. Some kidney tissue samples were then immersed in 10% (w/v) formalin for histopathological and immunohistochemical evaluation.

Histopathological examination

Tissues fixed in 10% (w/v) formalin were dehydrated in graded alcohol and embedded in paraffin. Masson's trichrome staining was performed according to the standard protocol by using a reagent kit purchased from Sigma (USA). For each section with Masson's trichrome, 10 fields were digitized and scanned at 400× magnification using imaging software (Photoshop, Adobe, San Jose, California). Using a grid superimposed on the image, the number of points overlapping the blue collagen staining was counted, and the percentage of blue collagen area in the examined tubulointerstitium was measured (Mizuguchi *et al*., 2004).

Immunostaining

For immunohistochemical analysis, paraffin sections (5 mm) were deparaffinized, washed with phosphate-buffered saline (PBS) and treated with 3% (v/v) H_2O_2 for 5 min. Sections were blocked with 10% (w/v) normal goat serum in Tris-HCl-buffered saline for 1 h and then incubated with primary antibodies, including rabbit antibodies to α-smooth muscle actin (α-SMA) (1:200, ABCAM, UK), rabbit antibodies to E-cadherin (1:200, Santa Cruz Biotechnology, Santa Cruz, CA, USA), mouse antibodies to thrombospondin-1 (TSP-1) (1:100, Neomarkers, Fremont, CA, USA) at 4 °C overnight. After washing, sections were incubated with appropriate biotin-conjugated secondary immunoglobulin G, and then treated with reagents from a Vecta-Elite streptavidin-peroxidase kit (Vector Laboratories, Burlingame, CA, USA) with a benzidine substrate for color development. Sections were counterstained with diluted hematoxylin. The scores were determined as previously reported (Fu *et al*., 2006). Briefly, the examined area of the tubulointerstitium was outlined, positive staining patterns were identified, and the percentage of positive area in the examined tubulointerstitium was measured. All scoring was performed in a blinded manner on coded slides.

Enzyme-linked immunosorbent assay (ELISA)

To measure the level of tissue active TGF-β1, kidney tissues were homogenized in the extraction buffer containing 20 mmol/L Tris-HCl (pH 7.5), 2 mol/L NaCl, 0.1% (w/v) Tween-80, 1 mmol/L ethylene diamine tetraacetic acid (EDTA), and 1 mmol/L phenylmethylsulfonyl fluoride, and the supernatant was removed after centrifugation at 19000×*g* for 20 min at 4 °C. Kidney tissue active TGF-β1 level was determined using a commercial Quantikine TGF-β1 ELISA kit in accordance with the protocol specified by the manufacturer (R & D Systems, USA).

Quantitative real-time reverse transcriptase polymerase chain reaction (RT-PCR) analysis

Total RNA was extracted using RNeasy Mini RNA Extracting Kit (QIAGEN, USA) according to the manufacturer's protocol. The yield and quality of the RNA were assessed by measuring the absorbance at 260 and 280 nm followed by electrophoresis on 1.5% (w/v) agarose gels. Total RNA (500 ng) was reverse-transcribed into complementary DNA (cDNA) with ExScript RT Reagent Kit (Perfect Real Time, Takara, Japan) according to the manufacturer's guideline. In order to accurately quantify the expression levels of α-SMA, TGF-β1, TSP-1, collagen I, and fibronectin, quantitative real-time RT-PCR with TaqMan probe technique was performed. Primers and probes of α-SMA, TGF-β1, TSP-1, collagen I, fibronectin, and the internal calibrator-glyceraldehyde-3-phosphate dehydrogenase (GAPDH) (synthesized by Sangon Biological Engineering Technology & Services Co., Shanghai, China) were listed in Table 1. A 30 μl PCR reaction solution (10× *Taq* buffer 3 μl; 25 mmol/L $MgCl_2$ 3 μl; 10 mmol/L dNTPs 1 μl; 10 μmol/L forward primer 1 μl; 10 μmol/L reverse primer 1 μl; 10 μmol/L TaqMan probe 1 μl; *Taq* DNA polymerase 1 U; cDNA 2 μl; diethyl pyrocarbonate (DEPC)-H_2O 17 μl) was amplified in Roche Lightcycler (Roche Diagnostics, USA). The thermocycle of PCR reaction was as follows: after an initial denaturation at 94 °C for 2 min, 45 cycles of

denaturation at 94 °C for 20 s, annealing at 54 °C for 20 s, and polymerization at 60 °C for 30 s were performed. PCR products went through agarose-gel electrophoretic analysis. During the real-time PCR process, fluorescence signal was collected during annealing steps. C_t (cycle of threshold) was calculated for further statistical analysis. In order to examine the efficiency of real-time PCR, standard curves were established with serial dilution of sample RNA (500 ng; α-SMA, TGF-β1, TSP-1, collagen I, fibronectin, GAPDH, 10× dilution). Pfaffl *et al*.(2002)'s method was used for the analysis of real-time PCR results.

Table 1 Oligonucleotide primer sets for real-time PCR

cDNA target	Oligonucleotide (5′→3′)
Collagen I	For.: TGG CGC TTC AGG TCC AAT
	Rev.: TGT TCC AGG CAA TCC ACG AG
	Pro.: 5′-FAM-CCA GCT TCC CCA TCA TCT CC-TAMRA-3′
Fibronectin	For.: CCA TTG CAA ATC GCT GCC AT
	Rev.: AAC ATT TCT CAG CTA TTG GCT T
	Pro.: 5′-FAM-CTC ATG TGG CCT CCT CCA C-TAMRA-3′
α-SMA	For.: GTT CGA AAC CTT CAA TGT TCC T
	Rev.: CAG TGC ATA GCC CTC GTA GAT
	Pro.: 5′-FAM-CCA TTC AAG CTG TGC TCT CGC T-TAMRA-3′
TGF-β1	For.: ACT ACT GCT TCA GCT CCA CA
	Rev.: GTG TCC AGG CTC CAA ATG T
	Pro.: 5′-FAM-CCA AGG GCT ACC ATG CCA AC-TAMRA-3′
TSP-1	For.: CCA CTG CAA AAA GGA CAA CTG
	Rev.: ATG GAC AGT TGT CCC TGT CAT
	Pro.: 5′-FAM-CCA TCC TTG TCA TAG TCT TCC TGC-TAMRA-3′
GAPDH	For.: CCT CAA GAT TGT CAG CAA T
	Rev.: CCA TCC ACA GTC TTC TGA GT
	Pro.: 5′-FAM-ACC ACA GTC CAT GCC ATC AC-TAMRA-3′

For., Rev., and Pro. indicate forward, reverse and probe, respectively. All primers and TaqMan probes were purchased from Sangon Biological Engineering Technology & Services Co. (Shanghai, China)

Western blot analysis

Protein from kidney tissues was extracted with RIPA (radio-immunoprecipitation assay) lysis buffer. After determination of protein concentrations, 20 μg of the protein was mixed with an equal amount of 2× sodium dodecyl sulfate (SDS) loading buffer for Western blot analysis as previously reported (Fu *et al*., 2006). Briefly, samples were heated at 99 °C for 5 min and then transferred to a polyvinylidene difluoride membrane. Nonspecific binding to the membrane was blocked for 1 h at room temperature with 5% (w/v) bovine serum albumin (BSA) in Tris-HCl-buffered saline. The membranes were then incubated overnight at 4 °C with primary antibodies, including rabbit antibodies to α-SMA (1:500, ABCAM, UK), rabbit antibodies to E-cadherin (1:500, Santa Cruz Biotechnology, Santa Cruz, CA, USA), mouse antibodies to TSP-1 (1:500, Neomarkers, Fremont, CA, USA), rabbit antibodies to phosphorylated Smad2 (pSmad2) (1:500, CST, USA) and β-actin (1:1000, Sigma, USA). After washing, the membrane was incubated with appropriate secondary immunoglobulin G-peroxidase conjugates (1:10000 dilution; KPL, USA), and developed using the enhanced chemiluminescence method. Band intensities were analyzed with Quantity One software. For quantification, the densities of α-SMA, E-cadherin, TSP-1 and pSmad2 were normalized to that of β-actin in the same sample.

Statistical analysis

All data were expressed as the mean±*SEM*. Statistical calculations were performed using the SPSS software (SPSS, Chicago, IL, USA). Inter-group comparisons were made by a one-way analysis of variance (ANOVA). The relationships between variables were assessed by Pearson correlation analysis. *P* values less than 0.05 were considered to be significant.

RESULTS

Ginsenoside Rg1 attenuated interstitial fibrosis in the obstructed kidney

It was shown by Masson's trichrome staining that there was no histological abnormality in sham-operated kidney (Fig.2a). On Day 7, the kidneys developed a conspicuous tubulointerstitial injury consisting of tubular dilatation and atrophy, interstitial inflammation and collagen accumulation. Tubulointerstitial damage was more prominent on Day 14 (Fig.2b). Administration of ginsenoside Rg1 markedly attenuated interstitial fibrosis and reduced the collagen accumulation on Days 7 and 14 after UUO ($P>0.05$ vs SOR on Day 7; $P<0.05$ vs SOR, $P<0.05$ vs UUO on Day 14) (Fig.2c, Table 2).

Table 2 Effect of ginsenoside Rg1 on interstitial fibrosis

Group	*n*	Interstitial collagen deposition (%)		Relative expression ratio of collagen I mRNA		Relative expression ratio of fibronectin mRNA	
		Day 7	Day 14	Day 7	Day 14	Day 7	Day 14
SOR	12	6.83±1.47	6.66±1.21	1	1	1	1
UUO	12	33.00±2.76$^{\Delta}$	57.00±2.76$^{\Delta}$	15.64±5.96$^{\Delta}$	22.11±8.33$^{\Delta}$	8.09±3.39$^{\Delta}$	16.95±7.42$^{\Delta}$
Rgl	12	8.89±2.07$^{\#}$	31.00±3.29*	7.38±2.06$^{\#}$	9.85±2.98*	3.03±1.48*	5.09±2.40*

$^{\Delta}P<0.05$ vs SOR control group; $^{\#}P>0.05$ vs SOR control group; $^{*}P<0.05$ vs UUO control group

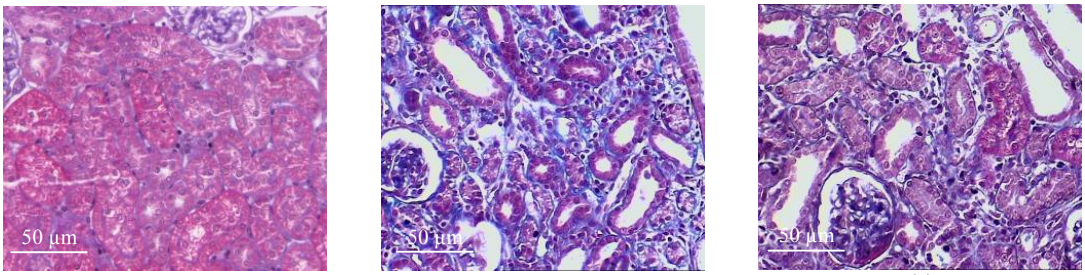

(a) (b) (c)

Fig.2 Masson's trichrome staining in all groups (14 d after UUO). (a) SOR; (b) UUO; (c) Rg1

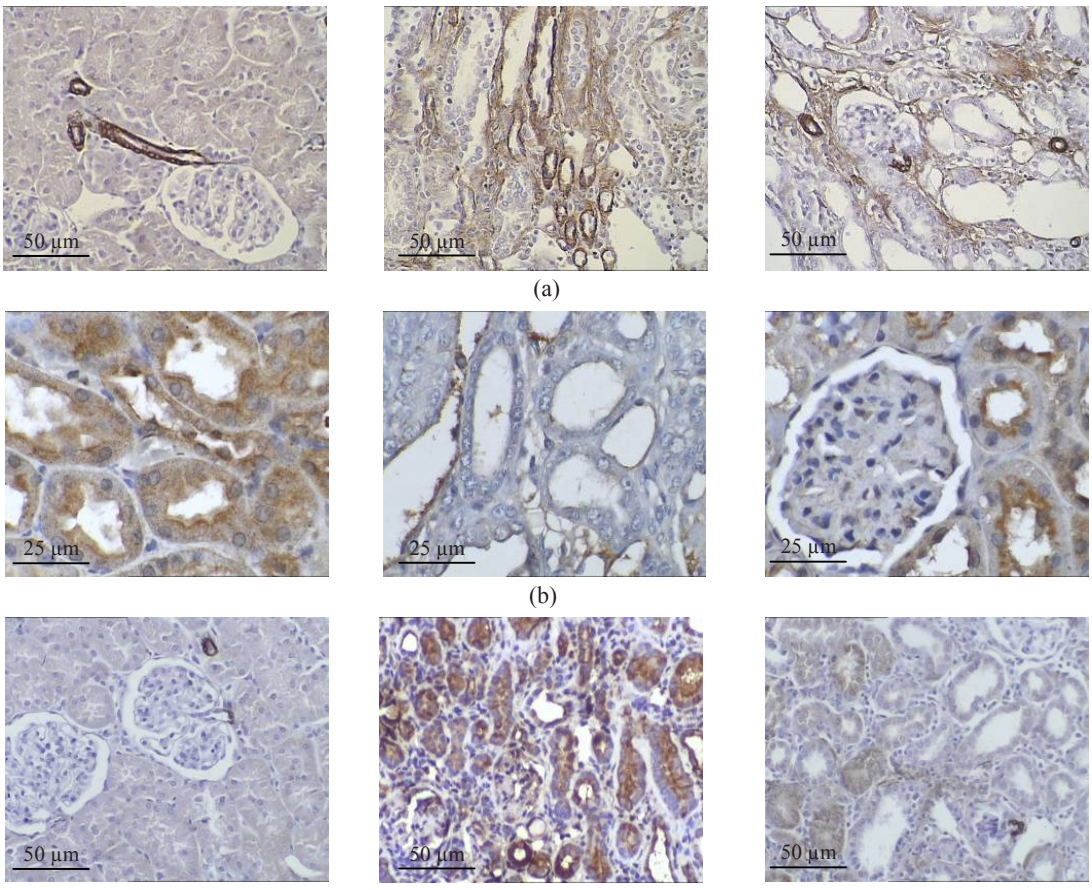

(a)

(b)

(c)

Fig.3 Immunohistochemical staining of (a) α-SMA (14 d after UUO), (b) E-cadherin (14 d after UUO), and (c) TSP-1 in all groups (7 d after UUO). Left: SOR; Middle: UUO; Right: Rg1

Collagen I and fibronectin are two major components of the interstitial matrix. As indicated by RT-PCR analysis, collagen I and fibronectin messenger RNA (mRNA) levels were increased substantially after UUO (P<0.05 vs SOR). Ginsenoside Rg1 treatment notably decreased these changes (P<0.05 vs SOR; P<0.05 vs UUO) (Table 2). These results further confirm that ginsenoside Rg1 could ameliorate renal interstitial fibrosis induced by UUO.

Effect of ginsenoside Rg1 on the expressions of α-SMA and E-cadherin in the obstructed kidney

α-SMA and E-cadherin are two commonly used markers for myofibroblast cell and epithelial cell, respectively. In the UUO model, increased expression of α-SMA and simultaneously decreased expression of E-cadherin often indicated TEMT. In the present experiment, the expression of α-SMA mRNA in the obstructed kidney increased dramatically on Days 7 and 14 after UUO (P<0.05 vs SOR), but decreased significantly after administration of ginsenoside Rg1 (P>0.05 vs SOR on Day 7; P<0.05 vs SOR, P<0.05, vs UUO on Day 14) (Table 3). Immunohistochemistry analysis indicated that the level of α-SMA in the obstructed kidney was increased obviously after UUO while the expression of E-cadherin decreased noticeably (P<0.05 vs SOR). Ginsenoside Rg1 treatment could significantly reverse these changes (Table 3, Figs.3a and 3b, see Page 889). These results are in accordance with Western blot analyses of α-SMA and E-cadherin (Fig.4). Taken together, these results suggest that UUO induced TEMT, which was significantly attenuated by ginsenoside Rg1.

Ginsenoside Rg1 decreased the expressions of TGF-β1 and pSmad2 in the obstructed kidney

TGF-β1 via activating Smad pathway (Smad2/3) plays an important role in the TEMT process and the pathogenesis of renal fibrosis. Therefore, in the next step of this study, the expressions of TGF-β1 and pSmad2 were investigated. On Days 7 and 14 after UUO, the expression of TGF-β1 mRNA in the obstructed kidney increased dramatically (P<0.05 vs SOR). However, administration of ginsenoside Rg1 significantly decreased the level of TGF-β1 mRNA in the obstructed kidney (P>0.05 vs SOR on Day 7; P<0.05 vs SOR, P<0.05 vs UUO on Day 14) (Table 4). Furthermore, in the obstructed kidney, quantitative analysis by specific ELISA exhibited approximately 3.2- and 2.4-fold increases in active TGF-β1 level, respectively, on Days 7 and 14 after UUO (P<0.05 vs SOR). However, ginsenoside Rg1 administration markedly reduced the increase of active TGF-β1 level in the obstructed kidney (P<0.05 vs SOR; P<0.05 vs UUO) (Table 4). Western blot analysis further verified that the pSmad2 was enhanced substantially on Days 7 and 14 after UUO in the obstructed kidney. However, ginsenoside Rg1 treatment significantly declined the enhancement of pSmad2 induced by UUO (Fig.4).

Ginsenoside Rg1 reduced the expression of TSP-1 in the obstructed kidney

As indicated by RT-PCR analysis, the expression of TSP-1 mRNA in the obstructed kidney increased notably on Days 7 and 14 after UUO (P<0.05 vs SOR), but decreased significantly after administration of ginsenoside Rg1 (P>0.05 vs SOR) (Table 5). TSP-1 protein was identified in nonobstructed kidneys in smooth muscle cells of the arterioles and arteries in rats (Fig.3c). TSP-1 was markedly increased in obstructed kidneys in cortical tubular epithelial cells on Days 7 and 14 (Fig.3c), but the expression was attenuated by ginsenoside Rg1 treatment (P<0.05 vs SOR; P<0.05 vs UUO) (Fig.3c, Table 5). These results are in accordant with Western blot analysis of TSP-1 (Fig.4).

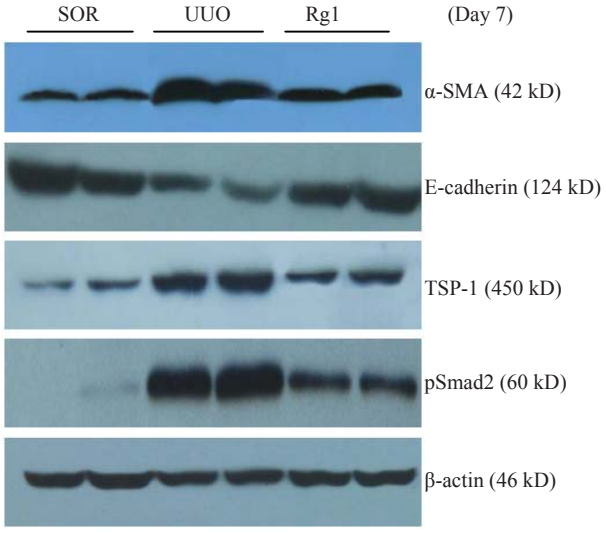

Fig.4 Western blot analyses of the expressions of α-SMA, E-cadherin, TSP-1, and pSmad2 normalized to β-actin in all groups

Table 3 Effect of ginsenoside Rg1 on renal TEMT

Group	*n*	Relative expression ratio of α-SMA mRNA		Immunohistochemistry analysis of α-SMA (%)		Immunohistochemistry analysis of E-cadherin (%)	
		Day 7	Day 14	Day 7	Day 14	Day 7	Day 14
SOR	12	1	1	1.67±1.21	2.17±1.17	36.33±4.22	35.67±4.58
UUO	12	8.00±3.34$^{\Delta}$	16.95±7.43$^{\Delta}$	22.67±2.73$^{\Delta}$	28.50±1.97$^{\Delta}$	24.17±2.79$^{\Delta}$	19.17±3.37$^{\Delta}$
Rgl	12	3.03±1.48$^{\#}$	5.09±2.39*	9.00±2.09*	14.00±1.55*	28.00±2.76$^{\#}$	28.00±4.69*

$^{\Delta}P<0.05$ vs SOR control group; $^{\#}P>0.05$ vs SOR control group; $^{*}P<0.05$ vs UUO control group

Table 4 Effect of ginsenoside Rg1 on expression of TGF-β1

Group	*n*	Relative expression ratio of TGF-β1 mRNA		Tissue active TGF-β1 level (pg/mg protein)	
		Day 7	Day 14	Day 7	Day 14
SOR	12	1	1	35.82±3.63	39.17±4.76
UUO	12	11.99±5.43$^{\Delta}$	11.31±4.60$^{\Delta}$	115.80±10.69$^{\Delta}$	92.10±9.18$^{\Delta}$
Rgl	12	3.36±1.93$^{\#}$	4.76±1.99*	51.09±4.75*	61.54±9.82*

$^{\Delta}P<0.05$ vs SOR control group; $^{\#}P>0.05$ vs SOR control group; $^{*}P<0.05$ vs UUO control group

Table 5 Effect of ginsenoside Rg1 on expression of TSP-1

Group	*n*	Relative expression ratio of TSP-1 mRNA		Immunohistochemistry analysis of TSP-1 (%)	
		Day 7	Day 14	Day 7	Day 14
SOR	12	1	1	2.92±1.20	3.08±1.43
UUO	12	7.90±2.29$^{\Delta}$	7.54±2.13$^{\Delta}$	24.50±3.20$^{\Delta}$	19.80±3.21$^{\Delta}$
Rgl	12	2.45±0.64$^{\#}$	2.30±0.62$^{\#}$	9.67±2.80*	10.67±3.27*

$^{\Delta}P<0.05$ vs SOR control group; $^{\#}P>0.05$ vs SOR control group; $^{*}P<0.05$ vs UUO control group

Correlation between TSP-1 and active TGF-β1 in the obstructed kidney

It was reported that antisense oligonucleotides against TSP-1 decrease the activation but not the expression of TGF-β1 in nephritic glomeruli (Daniel *et al*., 2003). Therefore, we evaluated the relationship between TSP-1 and active TGF-β1 in the current study. Pearson correlation analysis indicated that there was a significant positive correlation between the expression of TSP-1 and the level of active TGF-β1 (r=0.92, P<0.05) (Fig.5).

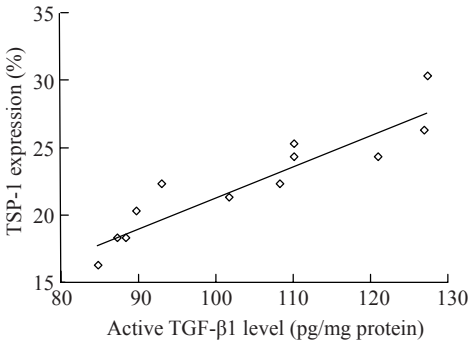

Fig.5 Correlation between TSP-1 expression and active TGF-β1 level

DISCUSSION AND CONCLUSION

Ginsenoside Rg1, a panaxatriol saponin, is one of the major active molecules from PNS. It is demonstrated that ginsenoside Rg1 can significantly attenuate the development of myocardial fibrosis as well as hepatic fibrosis (Wei *et al*., 2007; Wu *et al*., 2003). Ma *et al*.(2007) showed that in a rat model of hepatic fibrosis, panaxsaponin Rg1 protected hepatic function, degraded the levels of pCIII, HA, LN, and improved the pathological changes. Zhang and Wang (2006) demonstrated that ginsenoside Rg1 significantly inhibited the proliferation of human arterial smooth muscle cells (HASMCs) induced by tumor necrosis factor-α (TNF-α), and its antiproliferative effect involved in the inhibition of ERK and PI3K/PKB activation. These documents suggest that ginsenoside Rg1 may play a role in the prevention of tissue fibrosis. Data presented in this study indicated that ginsenoside Rg1 can potently attenuate renal

fibrosis in rats with UUO.

Consistent with other reports (Mizuguchi *et al*., 2004), after UUO, severe tubular atrophy, loss, dilation, infiltration of inflammatory cells and interstitial matrix deposition were noted. Importantly, we found that administration of ginsenoside Rg1 significantly blunted renal fibrosis induced by UUO, which included tubulointerstitial damage and collagen matrix accumulation.

Interstitial fibroblasts are the principal effector cells of renal fibrosis. Iwano *et al*.(2002) found that a large proportion of interstitial fibroblasts were actually originated from local TEMT during renal fibrogenesis. In the process of TEMT, tubular epithelial cells lose epithelial cell marker E-cadherin and *de novo* express myofibroblast cell marker α-SMA (Liu, 2004). Selective blockade of TEMT in a mouse genetic model dramatically reduces fibrotic lesions after obstructive injury, underscoring a definite importance of TEMT in renal fibrogenesis (Yang *et al*., 2002). In the present study, we demonstrated that there was a dramatic increase of α-SMA expression in the obstructed kidney after UUO. On the other hand, epithelial cell marker E-cadherin was substantially decreased in the tubular epithelium of the obstructed kidney. These data indicated that there existed marked transition from tubular epithelial cells into myofibroblasts in the obstructed kidney. Our studies confirm that administration of ginsenoside Rg1 largely decreased the expression of α-SMA and, meanwhile, increased the expression of E-cadherin. The results suggest that ginsenoside Rg1 could inhibit TEMT process in the UUO model. Previous studies from our laboratory show that PNS had an ameliorative effect on the fibrotic process of renal interstitium, and it could block TEMT in vivo (Su *et al*., 2005). The present results suggest that ginsenoside Rg1 has a comparable contribution to renal fibrosis and TEMT, which may be the most effective saponin in PNS against renal fibrosis.

We and other researchers have shown that TGF-β1 is the most potent inducer capable of initiating and completing the entire TEMT course (Fan *et al*., 1999; Liu, 2004), and that TGF-β1-induced TEMT appears to be primarily dependent on Smad pathway (activation of Smad2/3) (Liu, 2004; Wang *et al*., 2005). In the present study, the drastic increases of TGF-β1 mRNA and pSmad2 were observed in the obstructed kidney, which were considerably reversed by ginsenoside Rg1 treatment. Moreover, ginsenoside Rg1 also reduced the increased level of active TGF-β1 after UUO. Taken together, these results suggest that the effect of ginsenoside Rg1 on renal fibrosis induced by UUO may be associated with the inhibition of TGF-β1 and its Smad pathway.

TGF-β1, considered as the most potent inducer of TEMT, must be activated extracellularly before it can bind to its receptors. TSP-1 has been identified as the major activator of latent TGF-β1 in vitro and in vivo (Yevdokimova *et al*., 2001; Hugo, 2003; Naito *et al*., 2004; Daniel *et al*., 2003; 2004). In the present study, the levels of TSP-1 mRNA and protein in the obstructed kidney were notably increased compared with SOR, which is in agreement with observations in remnant kidney model (Hugo *et al*., 2002). Correlation analysis further showed that there was a positive correlation between TSP-1 and active TGF-β1 in the obstructed kidney, supporting the concept that TSP-1 played a major role in the activation of TGF-β1.

Yung *et al*.(2006) showed that the exogenous TSP-1 could increase TGF-β1 mRNA in a dose-dependent manner in human proximal renal tubular epithelial cells (HK-2 cells), and that TSP-1-mediated increase in TGF-β1 transcription was accompanied by increased TGF-β1 secretion and bioactivity. Our study reveals that, in the presence of ginsenoside Rg1, the increases of TGF-β1 mRNA, active TGF-β1 and TSP-1 were all suppressed. It appears reasonable to suggest that the beneficial effects of ginsenoside Rg1 in the UUO-induced renal interstitial fibrosis may be at least partly via decreasing the expression of TSP-1 and subsequently inhibiting the transcription and activation of TGF-β1. However, the exact mechanisms underlying the renoprotective effects of ginsenoside Rg1 need to be further elucidated.

In summary, we have demonstrated, to our knowledge for the first time, that ginsenoside Rg1 could inhibit renal interstitial fibrosis in rats with UUO. The beneficial effect of ginsenoside Rg1 might be related to the inhibition of TEMT via suppressing the expression of TSP-1 and then suppressing the transcription and activation of TGF-β1. Further studies are necessary to clarify the exact role of ginsenoside Rg1 on renal fibrosis.

References

Chan, R.Y., Chen, W.F., Dong, A., Guo, D., Wong, M.S., 2002. Estrogen-like activity of ginsenoside Rg1 derived from Panax notoginseng. *J. Clin. Endocrinol. Metab.*, **87**(8): 3691-3695. [doi:10.1210/jc.87.8.3691]

Daniel, C., Takabatake, Y., Mizui, M., Isaka, Y., Kawashi, H., Rupprecht, H., Imai, E., Hugo, C., 2003. Antisense oligonucleotides against thrombospondin-1 inhibit activation of TGF-beta in fibrotic renal disease in the rat in vivo. *Am. J. Pathol.*, **163**(3):1185-1192.

Daniel, C., Wiede, J., Krutzsch, H.C., Ribeiro, S.M., Roberts, D.D., Murphy-Ullrich, J.E., Hugo, C., 2004. Thrombospondin-1 is a major activator of TGF-beta in fibrotic renal disease in the rat in vivo. *Kidney. Int.*, **65**(2): 459-468. [doi:10.1111/j.1523-1755.2004.00395.x]

Fan, J.M., Ng, Y.Y., Hill, P.A., Nikolic-Paterson, D.J., Mu, W., Atkins, R.C., Lan, H.Y., 1999. Transforming growth factor-beta regulates tubular epithelial-myofibroblast transdifferentiation in vitro. *Kidney. Int.*, **56**(4):1455-1467. [doi:10.1046/j.1523-1755.1999.00656.x]

Fu, P., Liu, F., Su, S., Wang, W., Huang, X.R., Entman, M.L., Schwartz, R.J., Wei, L., Lan, H.Y., 2006. Signaling mechanism of renal fibrosis in unilateral ureteral obstructive kidney disease in ROCK1 knockout mice. *J. Am. Soc. Nephrol.*, **17**(11):3105-3114. [doi:10.1681/ASN.2005121366]

Guo, G., Morrissey, J., McCracken, R., Tolley, T., Liapis, H., Klahr, S., 2001. Contributions of angiotensin II and tumor necrosis factor-alpha to the development of renal fibrosis. *Am. J. Physiol. Renal. Physiol.*, **280**(5):F777-F785.

Hugo, C., 2003. The thrombospondin 1-TGF-beta axis in fibrotic renal disease. *Nephrol. Dial. Transplant.*, **18**(7): 1241-1245. [doi:10.1093/ndt/gfg159]

Hugo, C., Kang, D.H., Johnson, R.J., 2002. Sustained expression of thrombospondin-1 is associated with the development of glomerular and tubulointerstitial fibrosis in the remnant kidney model. *Nephron*, **90**(4):460-470. [doi:10.1159/000054735]

Iwano, M., Plieth, D., Danoff, T.M., Xue, C., Okada, H., Neilson, E.G., 2002. Evidence that fibroblasts derive from epithelium during tissue fibrosis. *J. Clin. Invest.*, **110**(3):341-350. [doi:10.1172/JCI200215518]

Li, L., Sheng, Y.X., Zhang, J.L., Wang, S.S., Guo, D.A., 2006. High-performance liquid chromatographic assay for the active saponins from Panax notoginseng in rat tissues. *Biomed. Chromatogr.*, **20**(4):327-335. [doi:10.1002/bmc.567]

Liu, Y., 2004. Epithelial to mesenchymal transition in renal fibrogenesis: pathologic significance, molecular mechanism, and therapeutic intervention. *J. Am. Soc. Nephrol.*, **15**(1):1-12. [doi:10.1097/01.ASN.0000106015.29070.E7]

Liu, Y., 2006. Renal fibrosis: new insights into the pathogenesis and therapeutics. *Kidney. Int.*, **69**(2):213-217. [doi:10.1038/sj.ki.5000054]

Ma, L.Q., Liang, B., Liu, B., Duan, L.P., Li, S.A., Dong, X.Q., Zhang, L., Zhan, E.Y., Yang, Z.W., Zhang, S.J., Wei, Y.M., Wu, X.J., Ji, D.G., 2007. Experimental study of Panaxsaponin Rg1 on hepatic fibrosis in rats. *Chin. J. Integr. Tradit. Western Med. Dig.*, **15**(3):165-168 (in Chinese).

Mizuguchi, Y., Miyajima, A., Kosaka, T., Asano, T., Asano, T., Hayakawa, M., 2004. Atorvastatin ameliorates renal tissue damage in unilateral ureteral obstruction. *J. Urol.*, **172**(6 Pt 1):2456-2459. [doi:10.1097/01.ju.0000138473.38447.f0]

Morrissey, J.J., Klahr, S., 1998. Differential effects of ACE and AT1 receptor inhibition on chemoattractant and adhesion molecule synthesis. *Am. J. Physiol.*, **274**(3 Pt 2): F580-F586.

Naito, T., Masaki, T., Nikolic-Paterson, D.J., Tanji, C., Yorioka, N., Kohno, N., 2004. Angiotensin II induces thrombospondin-1 production in human mesangial cells via p38 MAPK and JNK: a mechanism for activation of latent TGF-beta1. *Am. J. Physiol. Renal Physiol.*, **286**(2): F278-F287. [doi:10.1152/ajprenal.00139.2003]

Ng, T.B., 2006. Pharmacological activity of sanchi ginseng (Panax notoginseng). *J. Pharm. Pharmacol.*, **58**(8): 1007-1019. [doi:10.1211/jpp.58.8.0001]

Pfaffl, M.W., Horgan, G.W., Dempfle, L., 2002. Relative expression software tool (REST) for group-wise comparison and statistical analysis of relative expression results in real-time PCR. *Nucleic. Acids. Res.*, **30**(9):e36. [doi:10.1093/nar/30.9.e36]

Strutz, F., Müller, G.A., 2006. Renal fibrosis and the origin of the renal fibroblast. *Nephrol. Dial. Transplant.*, **21**(12): 3368-3370. [doi:10.1093/ndt/gfl199]

Su, B.H., Li, Z., Fan, J.M., Wang, M., Tang, R., 2005. Effects of Panax notoginseng saponins on the process of renal interstitial fibrosis after unilateral ureteral obstruction in rats. *Sichuan Da Xue Xue Bao Yi Xue Ban*, **36**(3):368-371 (in Chinese).

Wang, M., Fan, J.M., Liu, X.Y., 2004. Effect of total saponins of Panax notoginseng on transdifferentiation of rats' tubular epithelial cell induced by IL-1alpha. *Chin. J. Integr. Tradit. Western Med. Dig.*, **24**(8):722-725 (in Chinese).

Wang, W., Koka, V., Lan, H.Y., 2005. Transforming growth factor-beta and Smad signalling in kidney diseases. *Nephrology*, **10**(1):48-56. [doi:10.1111/j.1440-1797.2005.00334.x]

Wei, H.J., Yang, H.H., Chen, C.H., Lin, W.W., Chen, S.C., Lai, P.H., Chang, Y., Sung, H.W., 2007. Gelatin microspheres encapsulated with a nonpeptide angiogenic agent, ginsenoside Rg1, for intramyocardial injection in a rat model with infarcted myocardium. *J. Control. Rel.*, **120**(1-2): 27-34. [doi:10.1016/j.jconrel.2007.04.005]

Wu, F., Zhang, S.S., Kang, G.F., 2003. Effects of Panax notoginseng saponins on the expression of tumor necrosis factor alpha and secretion phospholipase A2 in rats with

liver fibrosis. *Zhonghua Gan Zang Bing Za Zhi*, **11**(1): 51-52 (in Chinese).

Yang, J., Shultz, R.W., Mars, W.M., Wegner, R.E., Li, Y., Dai, C., Nejak, K., Liu, Y., 2002. Disruption of tissue-type plasminogen activator gene in mice reduces renal interstitial fibrosis in obstructive nephropathy. *J. Clin. Invest.*, **110**(10):1525-1538. [doi:10.1172/JCI16219]

Yevdokimova, N., Wahab, N.A., Mason, R.M., 2001. Thrombospondin-1 is the key activator of TGF-beta1 in human mesangial cells exposed to high glucose. *J. Am. Soc. Nephrol.*, **12**(4):703-712.

Yung, S., Lee, C.Y., Zhang, Q., Lau, S.K., Tsang, R.C., Chan, T.M., 2006. Elevated glucose induction of thrombospondin-1 up-regulates fibronectin synthesis in proximal renal tubular epithelial cells through TGF-beta1 dependent and TGF-beta1 independent pathways. *Nephrol. Dial. Transplant.*, **21**(6):1504-1513. [doi:10.1093/ndt/gfl017]

Zhang, H.S., Wang, S.Q., 2006. Ginsenoside Rg1 inhibits tumor necrosis factor-alpha (TNF-alpha)-induced human arterial smooth muscle cells (HASMCs) proliferation. *J. Cell. Biochem.*, **98**(6):1471-1481. [doi:10.1002/jcb.20799]